

University of Groningen

Colorectal anastomotic leak

van Praagh, J B; de Wit, J G; Olinga, P; de Haan, J J; Nagengast, W B; Fehrmann, R S N; Havenga, K

Published in:
British Journal of Surgery

DOI:
[10.1093/bjs/znaa066](https://doi.org/10.1093/bjs/znaa066)

IMPORTANT NOTE: You are advised to consult the publisher's version (publisher's PDF) if you wish to cite from it. Please check the document version below.

Document Version
Publisher's PDF, also known as Version of record

Publication date:
2021

[Link to publication in University of Groningen/UMCG research database](#)

Citation for published version (APA):

van Praagh, J. B., de Wit, J. G., Olinga, P., de Haan, J. J., Nagengast, W. B., Fehrmann, R. S. N., & Havenga, K. (2021). Colorectal anastomotic leak: Transcriptomic profile analysis. *British Journal of Surgery*, 108(3), 326-333. <https://doi.org/10.1093/bjs/znaa066>

Copyright

Other than for strictly personal use, it is not permitted to download or to forward/distribute the text or part of it without the consent of the author(s) and/or copyright holder(s), unless the work is under an open content license (like Creative Commons).



The publication may also be distributed here under the terms of Article 25fa of the Dutch Copyright Act, indicated by the "Taverne" license. More information can be found on the University of Groningen website: <https://www.rug.nl/library/open-access/self-archiving-pure/taverne-amendment>.

Take-down policy

If you believe that this document breaches copyright please contact us providing details, and we will remove access to the work immediately and investigate your claim.

Downloaded from the University of Groningen/UMCG research database (Pure): <http://www.rug.nl/research/portal>. For technical reasons the number of authors shown on this cover page is limited to 10 maximum.

Colorectal anastomotic leak: transcriptomic profile analysis

J. B. van Praagh ¹, J. G. de Wit², P. Olinga ³, J. J. de Haan⁴, W. B. Nagengast², R. S. N. Fehrmann⁴ and K. Havenga^{1,*}

¹Department of Surgery, University of Groningen, University Medical Centre Groningen, Groningen, the Netherlands

²Department of Gastroenterology and Hepatology, University of Groningen, University Medical Centre Groningen, Groningen, the Netherlands

³Pharmaceutical Technology and Biopharmacy, Department of Pharmacy, University of Groningen, Groningen, the Netherlands

⁴Department of Medical Oncology, University of Groningen, University Medical Centre Groningen, Groningen, the Netherlands

*Correspondence to: Department of Surgery, University Medical Centre Groningen, University of Groningen, Hanzeplein 1, PO Box 30.001, 9700 RB Groningen, the Netherlands (e-mail: k.havenga@umcg.nl)

Presented to the 39th Annual Meeting of the Surgical Infection Society, Coronado, California, USA, June 2019, and Dutch Digestive Disease Days, Veldhoven, the Netherlands, October 2019

Abstract

Background: Anastomotic leakage in patients undergoing colorectal surgery is associated with morbidity and mortality. Although multiple risk factors have been identified, the underlying mechanisms are mainly unknown. The aim of this study was to perform a transcriptome analysis of genes underlying the development of anastomotic leakage.

Methods: A set of human samples from the anastomotic site collected during stapled colorectal anastomosis were used in the study. Transcriptomic profiles were generated for patients who developing anastomotic leakage and case-matched controls with normal anastomotic healing to identify genes and biological processes associated with the development of anastomotic leakage.

Results: The analysis included 22 patients with and 69 without anastomotic leakage. Differential expression analysis showed that 44 genes had adjusted $P < 0.050$, consisting of two upregulated and 42 downregulated genes. Co-functionality analysis of the 150 most upregulated and 150 most downregulated genes using the GenetICA framework showed formation of clusters of genes with different enrichment for biological pathways. The enriched pathways for the downregulated genes are involved in immune response, angiogenesis, protein metabolism, and collagen cross-linking. The enriched pathways for upregulated genes are involved in cell division.

Conclusion: These data indicate that patients who develop anastomotic leakage start the healing process with an error at the level of gene regulation at the time of surgery. Despite normal macroscopic appearance during surgery, the transcriptome data identified several differences in gene expression between patients who developed anastomotic leakage and those who did not. The expressed genes and enriched processes are involved in the different stages of wound healing. These provide therapeutic and diagnostic targets for patients at risk of anastomotic leakage.

Introduction

Anastomotic leakage occurs in approximately 10 per cent of patients who undergo colorectal resection with primary anastomosis. A leak is associated with prolonged hospital stay, reoperation, permanent ostomies, and even death^{1,2}. There is limited evidence for preventative measures, such as diverting ostomies, omentoplasties, and bowel preparation^{3–5}. Many factors increase the risk of anastomotic leakage: poor perfusion of the bowel, increased tension on the anastomosis, technically imperfect anastomosis, chronic use of immune suppressive agents, and comorbidity including diabetes or atherosclerosis^{6,7}. In addition, it has been shown that anastomotic leakage is associated with low microbial diversity and the presence of bacteria such as *Enterococcus faecalis* at the anastomotic site^{8,9}. However, the biological signalling pathways involved in normal or impaired

colonic wound healing and thus the pathophysiology of anastomotic leakage are incompletely understood.

Therefore, the aim of this study was to undertake a transcriptome analysis of genes underlying the development of colorectal anastomotic leakage.

Methods

The samples used for this study were obtained from patients who participated in the C-seal trial¹⁰. The trial was registered in the Netherlands National Trial Register (NTR3080). For patients who gave additional consent, the doughnuts, comprising small rings of colon and/or rectum cut by the circular stapler, were stored in RNeasy[®] (ThermoFisher Scientific, Waltham, Massachusetts, USA) at -80°C . Patients who developed anastomotic leak were

Received: April 04, 2020. Revised: July 17, 2020. Accepted: October 03, 2020

© The Author(s) 2021. Published by Oxford University Press on behalf of BJS Society Ltd. All rights reserved.

For permissions, please email: journals.permissions@oup.com

matched for sex, age, and preoperative chemotherapy and radiotherapy with patients who did not develop leakage.

RNA isolation

Total RNA was extracted from proximal doughnuts using a protocol involving a combination of bead beating and a Maxwell[®] 16 LEV simplyRNA Tissue Kit (Promega, Madison, Wisconsin, USA). Briefly, up to 60 mg tissue sample, 245 μ l 1-thioglycerol/Homogenization Solution (provided with kit) and minibeat glass beads were added to an Eppendorf tube and disrupted in a bead beater three times each for 45 s. Subsequently the homogenates were heated at 70°C for 2 min and cooled for 1 min. Samples were then centrifuged at 13 200g for 5 min, and 200 μ l supernatant transferred into new tubes with 200 μ l Kit Lysis Buffer. The samples were vortexed and transferred into Maxwell[®] 16 LEV Cartridge Purification Kit cartridges. An additional 10 μ l kit DNase I was added to the other wells of the cartridges as described by the protocol, and 40 μ l nuclease-free water was used for elution.

RNA quality check

Quantity and quality were assessed with a NanoDrop spectrophotometer (ThermoScientific). Only RNA samples with a 260/280 ratio of 1.9–2.1 and 260/230 ratio over 2.0 were used. Additional quality checking of the extracted total RNA and total RNA quantification of the samples was done by capillary electrophoresis using a LabChip GX (PerkinElmer, Waltham, Massachusetts, USA). Samples were included for further analysis if the 28S/18S ribosomal RNA ratio was greater than 0.8 and the mean RNA quality score exceeded 5.0.

Messenger RNA sequencing

Libraries of cDNA fragments were generated using BioScientific Nextflex mRNA sample preparation kits (BioScientific, Austin, Texas, USA) and a Sciclone NGS Liquid Handler (PerkinElmer). In the event of Sciclone contamination of adapter duplexes, an extra purification of the libraries was performed using a LabChip XT automated agarose gel separation system (PerkinElmer). The cDNA fragment libraries obtained from the samples were sequenced using a NextSeq500 System (Illumina, San Diego, California, USA), with a single-end read and a read length of 75 base pairs in four pools of 24 samples.

Quality control of sequencing data

Quality control was performed by sequenced read and by sample, and quality control metrics were calculated from the raw sequencing data by using FastQC/0.11.3-Java-1.7.0_80. Subsequently all reads were aligned to the reference genome *build 37 human ensemble* release 75, using HISAT/0.1.5-beta-goof-1.7.20 with default mode, allowing for two mismatches in the alignment¹¹. Gene-level quantification in raw counts was performed by HTSeq/0.6.1p1 using default settings, and Ensembl version 75 was used as gene annotation database¹².

Differential gene expression analysis

Differential expression of the genes was analysed using DESeq2 package in R version 3.4.3 (R Foundation for Statistical Computing, Vienna, Austria). First, genes that did not have at least three samples with normalized counts exceeding 10 were prefiltered¹³. Thereafter, differential analysis was performed, creating a list of upregulated and downregulated genes based on the log₂ fold change and *P* value¹³. In addition, *P* values were adjusted for multiple comparisons by use of the Benjamini–Hochberg false

discovery rate ($\alpha = 0.05$). Adjusted *P* < 0.050 was considered significant.

Heatmap and hierarchical clustering

A heatmap was created with the 150 most upregulated and 150 most downregulated genes based on the adjusted *P* value in the data set using the ClustVis tool¹⁴, which is available online. The clustering distances were based on Pearson correlation subtracted from 1, and the Ward linkage method was used.

Co-functionality network analysis

A guilt-by-association approach was used that predicts likely functions for genes based on gene co-regulation (manuscript in preparation). A description of the underlying method can be found in [Appendix S1](#). This framework enables researchers to create a comprehensive network of predicted functionalities of individual genes (<http://www.genetica-network.com>). Based on this framework, the likelihood of every gene set as defined in a selected database can be calculated. This results in a vector of *n* likelihoods for each individual gene. The number of gene sets in the selected database determines *n*. Next, the correlation between the vectors of likelihoods of the different genes is calculated. The GenetICA framework then shows a network of genes in which all genes have at least a correlation with another gene above, with a least one correlation above the selected threshold. When selecting a clustered network of genes, it shows the enriched function of the Gene Ontology Biological Process (GO BP) gene sets and its enrichment value (*Z*-transformed *P* values), considered significant when the *Z*-score is greater than 1.96. For the present data set, the 150 most upregulated and 150 most downregulated genes based on adjusted *P* value were used with a threshold of 0.600 to separate clusters of genes. Clusters with at least 10 genes were used to perform the enrichment studies adequately.

Results

The study was started with 123 doughnut samples; 29 of these were from patients who developed anastomotic leakage. After quality control of extracted RNA and sequencing results, the analysis was continued with 91 samples. Of these, 22 samples were from patients who developed anastomotic leakage within 30 days of surgery, except for one patient who developed a leak 40 days after operation, and 69 were from patients who did not develop anastomotic leakage ([Fig. S1](#)). Baseline characteristics for both groups included in subsequent analyses are shown in [Table 1](#). With the exception of BMI (*P* = 0.023), no significant differences were observed.

Genes with significant differential expression between anastomotic leak and non-leak samples

Four hundred and sixteen genes were significantly (*P* < 0.050) upregulated and 1479 were downregulated in samples from patients with anastomotic leakage compared with samples from those with no leak. Forty-four of these genes had adjusted *P* < 0.050, two upregulated and 42 downregulated genes ([Fig. 1](#) and [Table 2](#)). A list of all genes is available in [File S1](#).

Heatmap with hierarchical clustering

A heatmap of the top 150 most significantly upregulated and top 150 most significantly downregulated genes in patients who developed anastomotic leak is shown in [Fig. 2](#). Most (15 of 22) of the anastomotic leak samples had a similar pattern of gene expression, as they clustered together. Differences in upregulation and downregulation in the samples from patients who did or did not

Table 1 Patient characteristics

	Total (n = 91)	Anastomotic leakage (n = 22)	No anastomotic leakage (n = 69)	P [§]
Age (years)*	64.0 (10.3)	65.0 (10.5)	63.7 (10.3)	0.628 [¶]
Sex ratio (M : F)	64:27	17:5	47:22	0.442
BMI (kg/m ²) [†]	26.5 (24.0–29.4)	27.7 (24.8–31.2)	25.9 (23.8–28.2)	0.023
Indication for surgery				0.160
Colorectal cancer	85 (93)	22 (100)	63 (91)	
Diverticular disease	4 (4)	0 (0)	4 (6)	
Other	2 (2)	0 (0)	2 (3) [‡]	
Co-morbidities				
Cardiovascular	42 (46)	11 (50)	31 (45)	0.677
Pulmonary	14 (15)	5 (23)	9 (13)	0.278
Neurological	11 (12)	3 (14)	8 (12)	0.806
Gastrointestinal	21 (23)	6 (27)	15 (22)	0.598
Urogenital	16 (18)	6 (27)	10 (14)	0.175
Musculoskeletal	15 (16)	5 (23)	10 (14)	0.371
Endocrine	16 (18)	3 (14)	13 (19)	0.584
Infectious	1 (1)	0 (0)	1 (1)	0.589
Concomitant malignancy	17 (19)	4 (18)	13 (19)	0.951
Curatively treated	15 (16)	4 (18)	11 (16)	
ASA grade				0.262
I	18 (20)	7 (32)	11 (16)	
II	61 (67)	12 (55)	49 (71)	
III	12 (13)	3 (14)	9 (13)	
Chronic corticosteroid	1 (1)	0 (0)	1 (1)	0.589
Preoperative treatment				
Chemoradiotherapy, 50 Gy	19 (21)	4 (18)	15 (22)	0.721 [#]
Chemotherapy only	1 (1)	0 (0)	1 (1)	
Short-course radiotherapy, 25 Gy	31 (34)	7 (32)	24 (35)	0.798 [#]
With chemotherapy	2 (2)	0 (0)	2 (3)	
Diverting ileostomy	0 (0)	0 (0)	0 (0)	1.000 [#]
Diverting colostomy	5 (5)	1 (5)	4 (6)	0.823 [#]
Hartmann	1 (1)	0 (0)	1 (1)	
During surgery				
New ostomy	40 (44)	8 (36)	32 (46)	0.416
C-seal	47 (52)	13 (59)	34 (49)	0.428

Values in parentheses are percentages unless indicated otherwise; values are *mean (s.d.) and [†]median (i.q.r.). Co-morbidities are defined as disease under specialists' treatment. [‡]Adenoma and recurrent pelvic leiomyosarcoma. [§]Mann-Whitney U test, except [¶]Welch's t test and [#]Pearson χ^2 test.

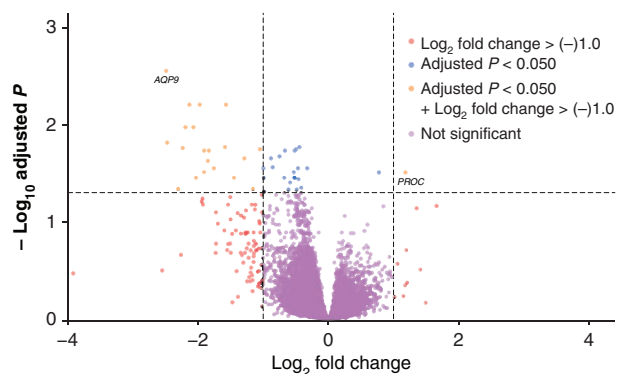


Fig. 1 Volcano plot showing distribution of gene expression patterns. The dotted lines are the adjusted P -value < 0.050 (horizontal) and the Log_2 fold change < -1.0 or > 1.0 (vertical).

develop anastomotic leak were seemingly dichotomous and were homogeneous within the groups, with the exception of three samples. These three samples (numbers 42, 118, and 123) belonged to the group without anastomotic leak, and showed a different, outlying pattern compared with other samples in this group. They showed greater upregulation in a subset of genes (MMP3 to TLR4) (Fig. 2).

Co-functionality network analysis

The GenetICA co-functionality network of the top 150 upregulated genes consisted of eight clusters of genes, ranging from 2 to

11 genes sharing predicted co-functionality. Only cluster 1 contained more than 10 genes (Fig. 3), showing enrichment of the pathways GO organelle fission (Z-score 5.60), GO transfer RNA metabolic process (Z-score 5.36), GO DNA repair (Z-score 5.31), GO amide biosynthetic process (Z-score 5.17), and GO non-coding RNA processing (Z-score 5.02). Because these pathways are related to cell division, this cluster 1 was labelled 'cell division' (Table S1).

The clusters formed by the downregulated genes consisted of 2 to 38 genes (Fig. 4). Three clusters contained more than 10 genes. Cluster 1 showed 37 genes that were enriched for pathways in the immune response, such as GO leucocyte activation (Z-score 7.77), GO defence response to bacterium (Z-score 6.98), and GO defence response to other organism (Z-score 6.94). Cluster 2 (16 genes) enriched for pathways that involve angiogenesis: GO vasculature development (Z-score 4.72), GO blood vessel morphogenesis (Z-score 4.34), and GO angiogenesis (Z-score 4.33). Cluster 3 (24 genes) enriched for pathways such as GO mRNA processing (Z-score 5.43), GO DNA repair (Z-score 5.33), and the pathway GO peptidyl lysine modification (Z-score 5.05). The pathways of cluster 3 are related to protein synthesis and collagen cross-linking (Table S2).

A subset of the downregulated genes in the immune response cluster were genes that were relatively downregulated owing to the three previously mentioned outlying samples. This subset of genes accounted for a large part of the enrichment of GO defence response to bacterium, GO inflammatory response, and GO defence response to other organism. These pathways had lower

Table 2 Genes that were differentially expressed between patients with or without anastomotic leakage (adjusted $P < 0.050$)

Gene symbol	Gene name	Log ₂ fold change	P	Adjusted P
Upregulated				
PROC	Protein C, inactivator of coagulation factors Va and VIIIa	1.182	4.35E-05	3.10E-02
RP4-740C4.7	RP4-740C4.7	0.776	4.48E-05	3.10E-02
Downregulated				
AQP9	Aquaporin 9	-2.489	1.41E-07	2.79E-03
HCAR3	Hydroxycarboxylic acid receptor 3	-2.473	5.38E-06	1.53E-02
MMP10	Matrix metalloproteinase 10	-2.305	9.41E-05	4.58E-02
PROK2	Prokineticin 2	-2.235	8.74E-06	1.74E-02
FCAR	Fc fragment of IgA receptor	-2.193	3.21E-06	1.06E-02
FCGR3B	Fc fragment of IgG receptor IIIb	-2.132	1.11E-06	6.22E-03
APOBEC3A	Apolipoprotein B mRNA editing enzyme catalytic subunit 3A	-2.070	2.91E-06	1.06E-02
LUCAT1	Lung cancer associated transcript 1	-2.030	6.35E-05	3.54E-02
CXCR2	C-X-C motif chemokine receptor 2	-1.973	1.15E-06	6.22E-03
CXCR1	C-X-C motif chemokine receptor 1	-1.905	1.35E-05	1.85E-02
MTRNR2L8	MT-RNR2-like 8	-1.905	4.52E-05	3.10E-02
FPR2	Formyl peptide receptor 2	-1.849	2.37E-05	2.35E-02
KCNJ15	Potassium voltage-gated channel subfamily J member 15	-1.833	1.40E-05	1.85E-02
MMP3	Matrix metalloproteinase 3	-1.757	3.53E-05	2.81E-02
SLC11A1	Solute carrier family 11 member 1	-1.586	7.23E-06	1.70E-02
CSF3R	Colony-stimulating factor 3 receptor	-1.570	1.25E-06	6.22E-03
FPR1	Formyl peptide receptor 1	-1.449	6.00E-05	3.54E-02
MGAM	Maltase-glucoamylase	-1.289	2.02E-05	2.22E-02
SELL	Selectin L	-1.157	9.45E-05	4.58E-02
SLC16A7	Solute carrier family 16 member 7	-1.051	1.08E-05	1.79E-02
EMP1	Epithelial membrane protein 1	-0.997	3.33E-05	2.81E-02
NAMPT	Nicotinamide phosphoribosyltransferase	-0.991	6.40E-05	3.54E-02
NAMPTL	Nicotinamide phosphoribosyltransferase-like	-0.986	1.09E-04	4.91E-02
RP11-443N24.1	RP11-443N24.1	-0.880	2.12E-05	2.22E-02
HGF	Hepatocyte growth factor	-0.855	2.90E-05	2.74E-02
ZBED6	Zinc finger BED-type containing 6	-0.749	1.81E-05	2.12E-02
SLC2A13	Solute carrier family 2 member 13	-0.678	6.07E-05	3.54E-02
IKZF2	IKAROS family zinc finger 2	-0.666	1.49E-05	1.85E-02
IL6ST	Interleukin 6 signal transducer	-0.612	9.88E-05	4.65E-02
N4BP2	NEDD4-binding protein 2	-0.588	7.55E-05	3.95E-02
JMJD1C	Jumonji domain containing 1C	-0.532	4.44E-05	3.10E-02
CHD1	Chromodomain helicase DNA-binding protein 1	-0.524	6.20E-05	3.54E-02
GPR126	G protein-coupled receptor 126	-0.522	6.24E-05	3.54E-02
AHR	Aryl hydrocarbon receptor	-0.518	5.87E-05	3.54E-02
AGO2	Argonaute 2, RISC catalytic component	-0.517	1.27E-05	1.85E-02
DOCK4	Dedicator of cytokinesis 4	-0.495	1.03E-05	1.79E-02
QSER1	Glutamine and serine rich 1	-0.488	1.01E-04	4.65E-02
SOCS4	Suppressor of cytokine signalling 4	-0.467	3.53E-05	2.81E-02
B4GALT6	β-1,4-Galactosyltransferase 6	-0.459	6.81E-05	3.66E-02
DENND4A	DENN domain containing 4A	-0.444	7.69E-06	1.70E-02
ZNF800	Zinc finger protein 800	-0.417	8.76E-05	4.47E-02
PCGF5	Polycomb group ring finger 5	-0.325	3.21E-05	2.81E-02

Z-scores (5.00 or less) when the subset genes were left out of the analysis. However, a cluster of genes that enriched for innate immune response-related pathways such as GO leucocyte activation (Z-score 9.52), GO activation of immune response (Z-score 7.23), and GO regulation of innate immune response (Z-score 6.90) were still present if these outliers were excluded from the enrichment analyses (Table S3).

Discussion

This study presents a unique transcriptome analysis of 91 human colonic samples from the anastomotic site and subsequent clinical outcome. Despite normal macroscopic appearance during surgery, the transcriptomic data identified several differences in gene expression between patients who developed anastomotic leak and those who did not. The majority of these genes were downregulated at the time of surgery in patients who developed an anastomotic leak. These genes are interesting individually but should be considered in the context of pathway regulation. A co-functionality network analysis identified three clusters of more

than 10 downregulated genes in patients who developed anastomotic leak that can be labelled with the themes: immune response (cluster 1), angiogenesis (cluster 2), and protein synthesis and collagen cross-linking (cluster 3). The upregulated genes comprised one cluster with more than 10 genes that seemed to be involved in cell division processes. This analysis of the transcriptomic level between patients who did or did not develop anastomotic leakage shows a multifactorial transcriptomic signature of samples obtained just before the process of wound healing starts.

The upregulated cluster of genes that seems to regulate cell division is also found in skin fibroblasts from patients with Ehlers-Danlos syndrome¹⁵. In this disorder, mainly collagen type V is affected negatively; this has a central role in fibrillogenesis and influences the activation of other collagen types^{16,17}. Although none of the studied patients had Ehlers-Danlos syndrome, a negative influence on collagen type V could impair creation of extracellular matrix. However, uncontrolled upregulated cell division could also indicate the presence of colorectal cancer cells¹⁸; however, all samples had a large macroscopic tumour-free resection margin.

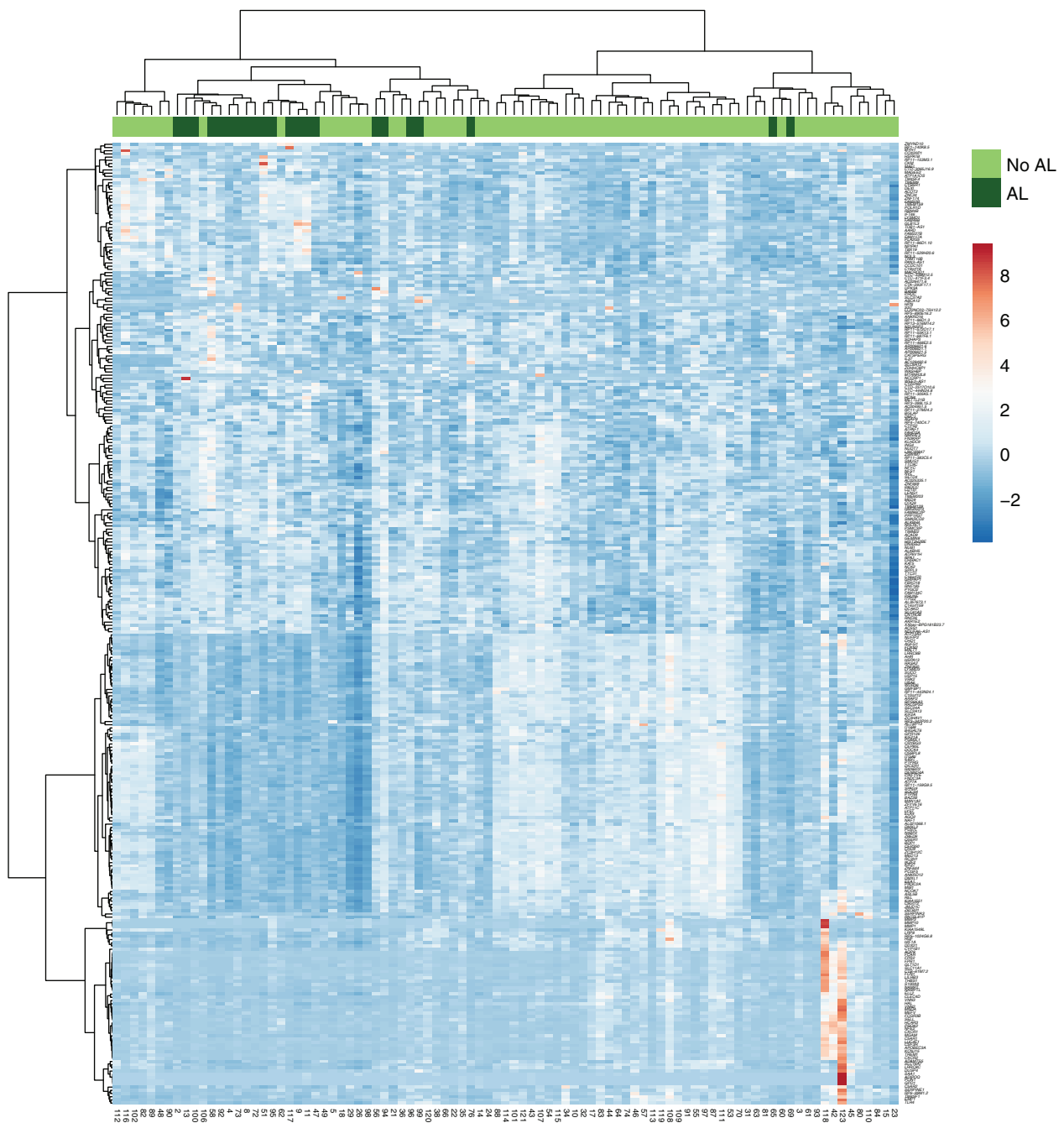


Fig. 2 Heatmap of differentially expressed genes with hierarchical clustering

The top 150 downregulated and top 150 upregulated genes are shown (rows) for each sample analysed (columns). The lower key refers to variance-stabilizing transformation of count data. AL, anastomotic leakage.

The identified downregulated gene clusters can all be related to wound healing, in which three stages are identified: inflammation, proliferation, and remodelling. There are no studies on the time course of normal intestinal healing; most analyses have focused on particular areas (such as epithelial cells) or diseased healing (for example inflammatory bowel disease)^{19,20}. However, from a biological viewpoint it is likely that wound healing processes in the human body largely work in the same way.

Transcriptomic analysis of different types of tissue has shown distinct activation and upregulation of genes involved in the immune and inflammatory response, especially in the early (inflammation) stages of healing^{21–23}. Compared with the normal wound healing response, the present results indicated that there

was downregulation of the innate immune response in patients who developed anastomotic leak *versus* those without a leak. The downregulation of gene sets related to the immune responses such as GO leucocyte activation and GO activation of immune response (immune response cluster) in an environment with an overabundance of microorganisms could cause an unfavourable situation for the healing colon after surgery and may be an important factor in development of anastomotic leakage.

However, the downregulated genes enriching for GO defence response to bacteria in anastomotic leak samples were mainly explained by high differential expression of three samples in the group without anastomotic leak. Although these samples seem to be outliers, the characteristics of the patients from whom they

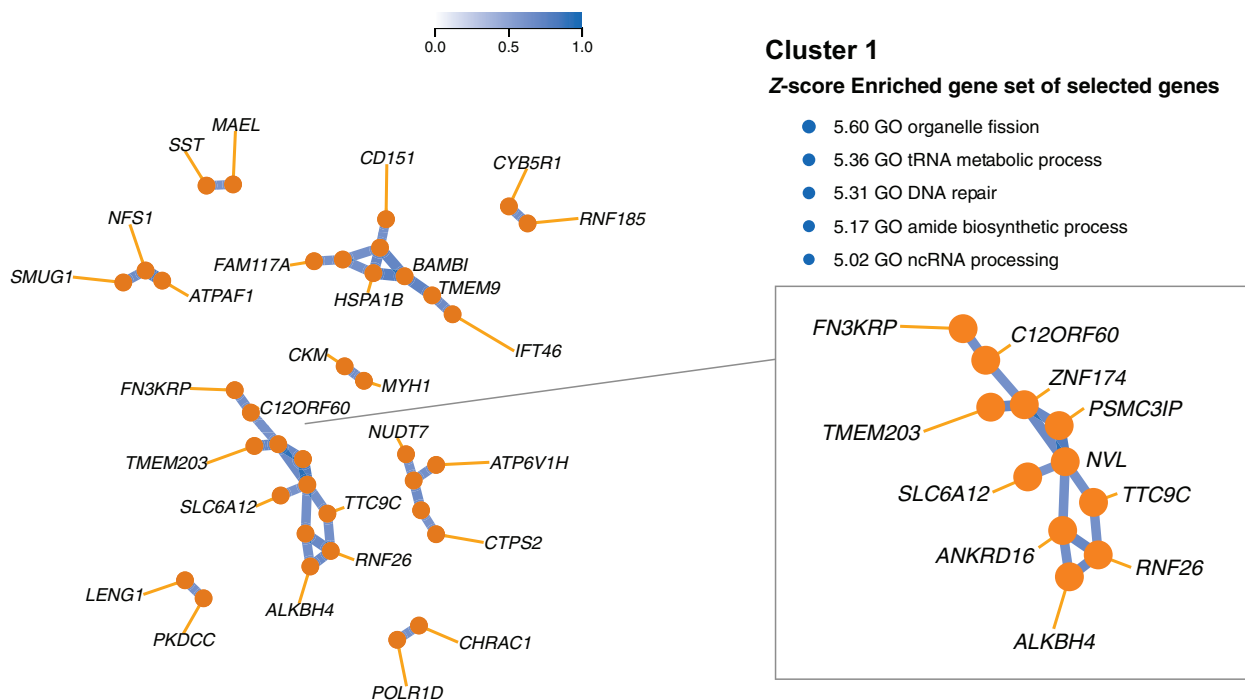


Fig. 3 Co-functionality network of top 150 upregulated genes within GO Biological Processes
 The threshold in the GenetiCA framework was set at 0.600. The network consists of nine different gene clusters sharing co-functionality, with the largest cluster containing 11 genes (cluster 1).

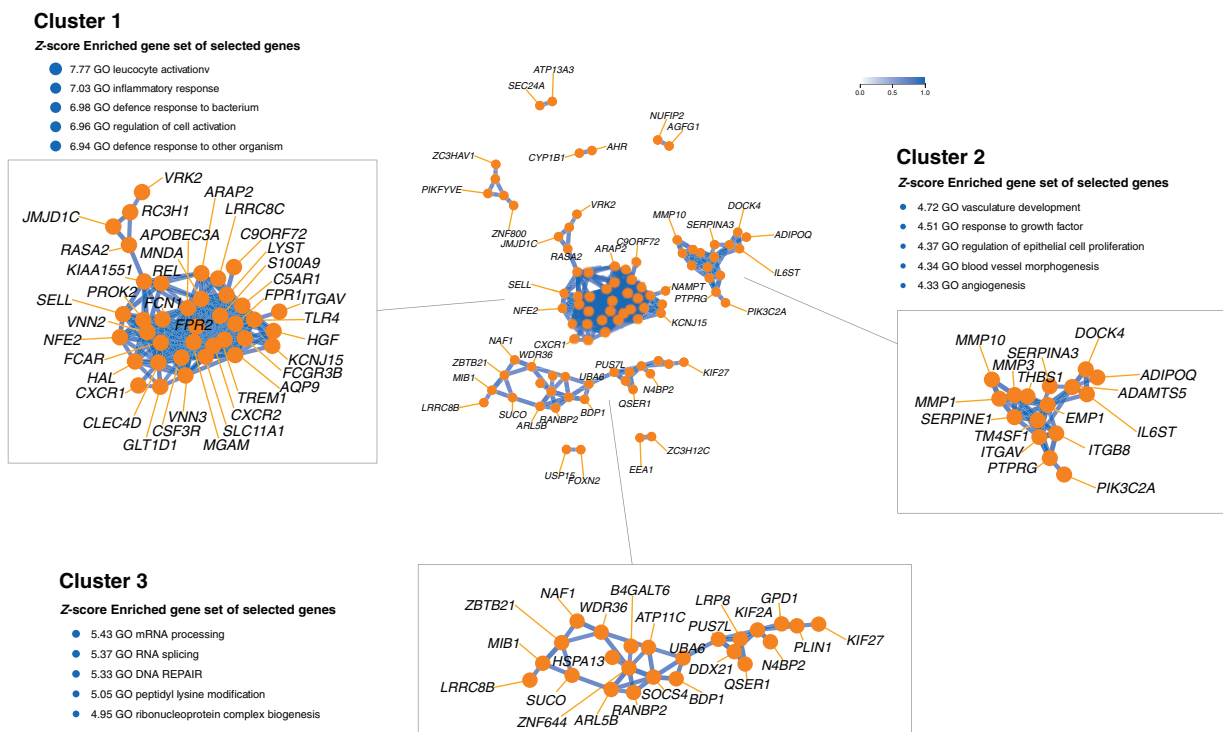


Fig. 4 Co-functionality network of top 150 downregulated genes within GO Biological Processes
 The threshold in the GenetiCA framework was set at 0.600. These genes aggregate in three larger clusters. Clockwise, the first and largest cluster (cluster 1) contains 38 genes, the second (cluster 2) consists of 16 genes, and cluster 3 consists of 24 genes.

were obtained were not divergent. It could be that these patients had such a high response to bacteria that they were unlikely to develop leakage caused by bacteria. Another explanation could be that a (larger amount of) lymph node was included in the doughnut.

The results also identified the angiogenesis cluster with down-regulated genes enriched for GO vasculature development and GO angiogenesis pathways, among others. Angiogenesis, resulting in adequate supply of oxygen and nutrients, is one of the pillars of the second, proliferative, phase of wound healing²⁴.

The healing of colonic anastomoses is considered to be more dependent on angiogenesis (microvasculature) than on oxygen diffusion through pre-existing macrovasculature^{25,26}. In addition, antiangiogenic agents have been associated with delayed wound healing and increased anastomotic leakage^{27,28}.

The third phase of wound healing, the remodelling phase, mainly comprises collagen restructuring. Anastomotic healing, which can be considered as secondary wound healing, starts with granulation. As the clotting matrix is transformed, a collagen network is formed, reducing the wound defect. Therefore, the balance of collagen production and fusion of the submucosal collagen matrix, which provides strength to the bowel, is an essential part of the healing of the anastomosis^{9,23,24}. Downregulation of the pathway GO peptidyl lysine modification, which is involved in collagen cross-linking²⁹, may therefore be another factor predisposing to anastomotic leakage.

There are several limitations to this study. First, only the proximal doughnut was used as the distal one was needed for pathological evaluation. It was therefore not possible to look at the downstream protein levels. In addition, the data would have had more impact if they also included information on microbial gene expression. The predictive value of the gene signatures in the present study is debatable, but this work provides new directions in the search for the mechanisms underpinning anastomotic leakage. Future work should focus on the biological status of the patient. From these data it has been possible to identify genes and biological routes that could be targeted for modulation or guided imaging. These could be used for risk profiling or even prediction of the development of anastomotic leak. However, confirmatory studies with a larger sample size, including preoperative samples, should be performed. Future in-depth analyses of the influences of different cell types using techniques such as microdissection could help improve understanding of the mechanisms underlying healing and thus leakage. A follow-up study using metatranscriptomics to analyse the gene expression of both host and microbes is planned.

Although there is no literature on how the pathways behave as soon as anastomotic wound healing has started, the hypothesis based on the present findings is that patients who eventually develop anastomotic leak start the healing process with an error. These patients have a status or trait at the level of gene regulation at the time of surgery that predisposes them to anastomotic leak. This predisposition is mainly based on the immune response, angiogenesis, protein metabolism, and collagen cross-linking, all of which are seemingly involved in the different stages of wound healing.

Disclosure. The authors declare no conflict of interest.

Supplementary material

Supplementary material is available at BJS online.

References

- Buchs NC, Gervaz P, Secic M, Bucher P, Mugnier-Konrad B, Morel P. Incidence, consequences, and risk factors for anastomotic dehiscence after colorectal surgery: a prospective monocentric study. *Int J Colorectal Dis* 2008;**23**:265–270
- Hammond J, Lim S, Wan Y, Gao X, Patkar A. The burden of gastrointestinal anastomotic leaks: an evaluation of clinical and economic outcomes. *J Gastrointest Surg* 2014;**18**:1176–1185
- Wong NY, Eu KW. A defunctioning ileostomy does not prevent clinical anastomotic leak after a low anterior resection: a prospective, comparative study. *Dis Colon Rectum* 2005;**48**:2076–2079
- Matthiessen P, Hallböök O, Rutegård J, Simert G, Sjødahl R. Defunctioning stoma reduces symptomatic anastomotic leakage after low anterior resection of the rectum for cancer: a randomized multicenter trial. *Ann Surg* 2007;**246**:207–214
- Rollins KE, Javanmard-Emamghissi H, Acheson AG, Lobo DN. The role of oral antibiotic preparation in elective colorectal surgery: a meta-analysis. *Ann Surg* 2019;**270**:43–58
- McDermott FD, Heeney A, Kelly ME, Steele RJ, Carlson GL, Winter DC. Systematic review of preoperative, intraoperative and postoperative risk factors for colorectal anastomotic leaks. *Br J Surg* 2015;**102**:462–479
- Nikolian VC, Kamdar NS, Regenbogen SE, Morris AM, Byrn JC, Suwanabol PA *et al*. Anastomotic leak after colorectal resection: a population-based study of risk factors and hospital variation. *Surgery* 2017;**161**:1619–1627
- van Praagh JB, de Goffau MC, Bakker IS, van Goor H, Harmsen HJM, Olinga P *et al*. Mucus microbiome of anastomotic tissue during surgery has predictive value for colorectal anastomotic leakage. *Ann Surg* 2019;**269**:911–916
- Shogan BD, Belogortseva N, Luong PM, Zaborin A, Lax S, Bethel C *et al*. Collagen degradation and MMP9 activation by *Enterococcus faecalis* contribute to intestinal anastomotic leak. *Sci Transl Med* 2015;**7**:286ra68
- Bakker IS, Morks AN, Ten Cate Hoedemaker HO, Burgerhof JGM, Leuvenink HG, Van Praagh JB *et al*. Randomized clinical trial of biodegradable intraluminal sheath to prevent anastomotic leak after stapled colorectal anastomosis. *Br J Surg* 2017;**10**:587–1019
- Kim D, Langmead B, Salzberg SL. HISAT: a fast spliced aligner with low memory requirements. *Nat Methods* 2015;**12**:357–360
- Anders S, Pyl PT, Huber W. HTSeq—a Python framework to work with high-throughput sequencing data. *Bioinformatics* 2015;**31**:166–169
- Love MI, Huber W, Anders S. Moderated estimation of fold change and dispersion for RNA-seq data with DESeq2. *Genome Biol* 2014;**15**:550
- Metsalu T, Vilo J. ClustVis: a web tool for visualizing clustering of multivariate data using principal component analysis and heatmap. *Nucleic Acids Res* 2015;**43**:W566–W570
- Chiarelli N, Carini G, Zoppi N, Ritelli M, Colombi M. Molecular insights in the pathogenesis of classical Ehlers–Danlos syndrome from transcriptome-wide expression profiling of patients' skin fibroblasts. *PLoS One* 2019;**14**:e0211647
- Sun M, Chen S, Adams SM, Florer JB, Liu H, Kao WWY *et al*. Collagen V is a dominant regulator of collagen fibrillogenesis: dysfunctional regulation of structure and function in a corneal-stroma-specific Col5a1-null mouse model. *J Cell Sci* 2011;**124**:4096–4105
- Wenstrup RJ, Florer JB, Brunskill EW, Bell SM, Chervoneva I, Birk DE. Type V collagen controls the initiation of collagen fibril assembly. *J Biol Chem* 2004;**279**: 53 331–53 337
- Guo Y, Bao Y, Ma M, Yang W. Identification of key candidate genes and pathways in colorectal cancer by integrated bioinformatical analysis. *Int J Mol Sci* 2017;**18**:722
- Haberman Y, Kams R, Dexheimer PJ, Schirmer M, Somekh J, Jurickova I *et al*. Ulcerative colitis mucosal transcriptomes reveal mitochondriopathy and personalized mechanisms underlying disease severity and treatment response. *Nat Commun* 2019;**10**:38
- Holgersen K, Kutlu B, Fox B, Serikawa K, Lord J, Hansen AK *et al*. High-resolution gene expression profiling using RNA

- sequencing in patients with inflammatory bowel disease and in mouse models of colitis. *J Crohns Colitis* 2015;**9**:492–506
21. St Laurent G, Seilheimer B, Tackett M, Zhou J, Shtokalo D, Vyatkin Y et al. Deep sequencing transcriptome analysis of murine wound healing: effects of a multicomponent, multitarget natural product therapy-Tr14. *Front Mol Biosci* 2017;**4**:57
 22. Sass PA, Dąbrowski M, Charzyńska A, Sachadyn P. Transcriptomic responses to wounding: meta-analysis of gene expression microarray data. *BMC Genomics* 2017;**18**:850
 23. Wang Y, Tatakis DN. Human gingiva transcriptome during wound healing. *J Clin Periodontol* 2017;**44**:394–402
 24. Thompson SK, Chang EY, Jobe BA. Clinical review: healing in gastrointestinal anastomoses, Part I. *Microsurgery* 2006;**26**:131–136
 25. Thornton FJ, Barbul A. Healing in the gastrointestinal tract. *Surg Clin North Am* 1997;**77**:549–573
 26. Shakhsher BA, Lec B, Zaborin A, Guyton K, Defnet AM, Bagrodia N et al. Lack of evidence for tissue hypoxia as a contributing factor in anastomotic leak following colon anastomosis and segmental devascularization in rats. *Int J Colorectal Dis* 2017;**32**:539–547
 27. te Velde EA, Voest EE, van Gorp JM, Verheem A, Hagendoorn J, Gebbink MF et al. Adverse effects of the antiangiogenic agent angiostatin on the healing of experimental colonic anastomoses. *Ann Surg Oncol* 2002;**9**:303–309
 28. Scappaticci FA, Fehrenbacher L, Cartwright T, Hainsworth JD, Heim W, Berlin J et al. Surgical wound healing complications in metastatic colorectal cancer patients treated with bevacizumab. *J Surg Oncol* 2005;**91**:173–180
 29. Yamauchi M, Sricholpech M. Lysine post-translational modifications of collagen. *Essays Biochem* 2012;**52**:113–133